ELSEVIER

Polymer 42 (2001) 431–441

polymer

www.elsevier.nl/locate/polymer

Photopolymerizable liquid encapsulants for microelectronic devices

K.K. Baikerikar[a], A.B. Scranton[b,*]

[a]*Department of Chemical Engineering, Michigan State University, 2527 Engineering Building, East Lansing, MI 48824, USA*
[b]*Department of Chemical and Biochemical Engineering, University of Iowa, 125 Chemistry Building, Iowa City, IA 52242, USA*

Received 22 June 1999; received in revised form 3 May 2000; accepted 10 May 2000

Abstract

Photopolymerizable liquid encapsulants (PLEs) for microelectronic devices may offer important advantages over traditional transfer molding compounds, including reduced in-mold cure times, lower thermal stresses, and reduced wire sweep. In this contribution, we discuss an encapsulation process based upon a low-viscosity resin that cures rapidly upon exposure to UV light. These highly filled PLEs are comprised of an epoxy novolac-based vinyl ester resin (~25 wt.%), fused silica filler (70–74 wt.%), photoinitiator, silane coupling agent, and, in some cases, a thermal initiator. We have characterized the degree of cure, flexural strength, flexural modulus, coefficient of thermal expansion, glass transition temperature, and thermal stress parameter of these novel PLEs. In addition, we investigated the effect of the fused silica loading, UV illumination time, and postcure time on these properties. The results indicate that a photocurable encapsulant containing 74.0 wt.% fused silica is very promising for microelectronic encapsulation. These liquid encapsulants cure (to an ejectable hardness) in less than 2 min for an initiating light intensity of 200 mW/cm^2 and exhibit appropriate values for the thermal and mechanical properties listed above.

Keywords: Photopolymerization; Liquid encapsulant; Microelectronic packaging

1. Introduction

1.1. Importance of semiconductor packaging

As the feature sizes on a semiconductor chip are reduced, the probability of contamination or damage (by scratching, handling, corrosion, etc.) is dramatically increased, and consequently there is a drastic reduction in the yield of the process [1–3]. For this reason, microelectronic devices are encapsulated in a plastic or ceramic package to protect the chip from physical and chemical damage. Another consequence of the increasingly large integration of features on a chip is the use of smaller and finer wires to electrically connect the semiconductor chip to the leadframe. During the encapsulation of microelectronic devices by the transfer molding process, these extremely fine wires are subjected to flow stresses from the molding compound and may be deformed or displaced (a phenomenon known as wire sweep). If the deformation of a bonding wire during encapsulation is sufficiently large, it may cause a short circuit (due to adjacent wires touching) or an open circuit (due to wires breaking) [4]. Thus, minimizing wire sweep during encapsulation is of prime importance, and is becoming more critical due to the use of an increasing number of wires in microelectronic packaging.

The process of chip encapsulation is particularly important since the chip has already undergone numerous processing steps and is just a few steps away from being a finished product (and thus has considerable value that is lost if the encapsulation step fails). With the currently used transfer molding process, it is very difficult to control the problem of wire sweep in a high pin count, fine pitch package. New trends in die design and packaging pose an increasing challenge to the wire sweep problem [2,3]. Indeed, due to the continuing advances in device capabilities and rapid changes in circuit board assembly methods, the packaging step is more important than ever before, and may, for the first time, impose limits on the design and performance of the final microelectronic device [5].

Microelectronic devices are typically encapsulated in a protective thermoset body from which a number of leads extend to allow electrical contact and interconnection between the encapsulated microelectronic device and a printed circuit board. Encapsulation of microelectronic devices has traditionally been accomplished using a transfer molding process. In this process, the thermoset molding compound (typically a solid epoxy preform) is dielectrically preheated and then placed into the pot of the molding tool. A transfer cylinder, or plunger, is used to push the molding

* Corresponding author. Tel.: +1-319-335-1414; fax: +1-319-335-1415.
E-mail address: elec-scranton@uiowa.edu (A.B. Scranton).

0032-3861/01/$ - see front matter
PII: S0032-3861(00)00388-8

compound into the runner system and gates of the mold [5]. The molding compound then flows over the chips, wirebonds, and leadframes, encapsulating the microelectronic device. The in-mold cure time is typically 2–3 min at 170°C. After they are ejected from the mold, the encapsulated microelectronic devices are postcured for 4–8 h at 170°C.

Most transfer molding processes suffer from significant problems arising from high operating temperatures (the molding compound is a solid at room temperature) and high pressures required to fill the mold (even in the melt state, the molding compound has a high viscosity, and the viscosity increases further with reaction). These aspects of the current process can lead to incomplete mold filling, thermal stresses (since the reaction temperature is much higher than the final use temperature), and wire sweep. Therefore, current transfer molding processes are plagued by two important problems: (i) wire sweep due to the high initial melt viscosity, and (ii) inadequate time to fill the mold due to rapid cure (concurrent with mold-filling) at the elevated operating temperatures. As the package sizes and the associated wires shrink to smaller and smaller dimensions, so does the operating window for transfer molding; hence, it is difficult to control wire sweep in the high pin count, fine pitch packages. These problems lead to productivity decreases due to increased packaging-related rejects for these new fine pitch microelectronic devices.

In our research, we are investigating a new strategy for microelectronic encapsulation using photopolymerizable liquid encapsulants. These highly filled PLEs are comprised of an epoxy novolac-based vinyl ester resin (~25 wt.%), fused silica (70–74 wt.%), and small amounts of a photoinitiator, silane coupling agent, and in some cases, a thermal initiator. For these PLEs, the use of light rather than heat to initiate the polymerization allows precise control over when the reaction starts, and therefore completely decouples the mold filling and the cure. The relatively low viscosity of the PLE allows low operating pressures and minimizes problems associated with wire sweep. Because photoinitiation allows active centers to be formed rapidly at room temperature, the in-mold cure time for the PLEs is no longer than the in-mold cure times of current transfer molding compounds.

In recent years, a number of investigators (including our research group) have demonstrated the feasibility of photopolymerization for curing thick polymers and composites [6,7]. In addition, Hanneman et al. [8] recently demonstrated the feasibility of using photopolymerizations to produce molded acrylate parts. These authors molded unfilled poly(methylmethacrylate) and found that they could produce high-quality parts more than 5 mm thick. In a previous publication on PLEs [9], we investigated the effect of the fused silica particle size distribution on the viscosity of PLEs for microelectronic applications. We characterized the viscosity of highly filled PLEs containing 70.0, 72.0, and 74.0 wt.% fused silica, and found that a broad particle size distribution obtained by mixing two fused silica distributions (one with a volume average particle size of ~10 μm and a second with an average size of ~30 μm) resulted in the best viscosity reduction. In addition, the PLE viscosity decreased slightly with increasing concentration of a silane coupling agent.

In this paper, we report an extensive series of studies on the thermal and mechanical properties, as well as, the degree of cure of photopolymerized liquid encapsulants. We have characterized the flexural strength, flexural modulus, coefficient of thermal expansion, glass transition temperature, and thermal stress parameter of PLEs containing 70.0–74.0 wt.% fused silica. We have also investigated the effects of the illumination time, postcure time, fused silica loading, and the inclusion of a thermal initiator on these thermal and mechanical properties of the final cured encapsulants.

2. Materials and methods

2.1. Photocurable encapsulant formulation

The photopolymerizable liquid encapsulant is comprised of a base resin, fused silica filler, photoinitiator, silane coupling agent, and in some cases a thermal initiator. The base resin used in these studies was an epoxy novolac-based vinyl ester resin (DERAKANE 470-45, Dow Chemical) that was chosen for its low initial viscosity (0.0456 Pa s or 45.6 cP at 25°C), as well as, its appropriate thermal and mechanical properties upon cure. The photoinitiator used was bis(2,4,6-trimethylbenzoyl) phenylphosphine oxide (IRGACURE 819, Ciba). This photoinitiator, which we will henceforth denote as BAPO, has been shown to be especially appropriate for curing relatively thick polymers and composites due to its efficient photobleaching [6,7]. In some systems, the thermal initiator, benzoyl peroxide (Aldrich), was used in order to investigate the effects of a dual photo/thermal initiation scheme on the resulting material properties of the encapsulant. The fillers used were crushed (angular), untreated fused silica obtained from MINCO, Inc. A silane coupling agent, 3-methacryloxypropyltrimethoxysilane (Z-6030, Dow Corning), was used to provide a stable bond between the base resin and the fused silica filler, and to improve the processability of the liquid encapsulant formulation.

Fused silica, which is the most common filler for commercial microelectronic encapsulants, was selected for these experiments because it possesses the optimum combination of properties. Specifically, it exhibits a low coefficient of thermal expansion ($\sim 0.6 \times 10^{-6} °C^{-1}$) and a low enough abrasiveness to provide a relatively long molding tool lifetime, especially when compared to aluminum nitride [5]. In addition, fused silica is transparent to UV light, and is therefore appropriate for UV curing [10]. To minimize the viscosity of the PLE, fused silica products with two different particle size distributions were used: (i) MIN-SIL 40 (volume average particle size = 32.42 μm,

median particle size = 22.11 μm) and (ii) MIN-SIL 550 (volume average particle size = 10.37 μm, median particle size = 6.026 μm). In our previous research, we found that PLEs in which the filler was comprised of a 50:50 wt.% blend of MIN-SIL 40 and MIN-SIL 550 provided the best rheological properties and processability [9]. For example, the PLE utilizing this blend and filled with 70.0 wt.% fused silica has a viscosity of 5.92 Pa s (5920 cP) at room temperature and the 72.0 wt.% PLE has a viscosity of 13.9 Pa s (13,900 cP), while the 74.0 wt.% PLE has a viscosity over 30.0 Pa s (30,000 cP). These viscosities are lower than those exhibited by traditional transfer molding compounds, which can range from 15 to 100 Pa s. Therefore, this 50:50 blend of MIN-SIL 40 and MIN-SIL 550 has been used for all of the PLEs in this investigation.

The PLEs were prepared by adding 0.2 wt.% BAPO photoinitiator (based on resin weight) to the epoxy novolac-based vinyl ester resin and stirring at room temperature on a magnetic stir plate until the photoinitiator completely dissolved (~3 min). This amount of photoinitiator was selected because it was demonstrated in an earlier work to be the optimal concentration with regard to the final properties obtained [7]. In some cases, 1.2 wt.% (based on resin weight) of the thermal initiator, benzoyl peroxide, was also added and again the system was stirred until dissolution was complete (~8 min). The silane coupling agent was added dropwise to the desired 1 wt.% (based on filler weight) and the resin mixture was stirred on the magnetic stir plate. Fused silica was added in the amount of 70.0, 72.0, or 74.0 wt.% and the system mixed by using a vortex mixer until the filler was completely dispersed and a homogeneous mixture was achieved. The PLE was then degassed in a vacuum oven. Once these steps were completed, the PLE was ready to use for preparing samples required for the material property characterization studies.

2.2. Flexural strength and modulus

Specimens for flexural testing were prepared by photopolymerizing the liquid encapsulant in rectangular silicone molds with unfiltered UV light (200 mW/cm^2 UVA intensity) from a 3000 W arcless mercury vapor lamp (Fusion UV Systems, model F450T). Light intensities were measured (over the 320–390 nm range) using a UVICURE Plus high energy UV integrating radiometer. The specimens were 76.2 mm long, 12.7 mm wide, and 3.2 mm deep. To investigate the effect of the illumination time, the samples were illuminated for 60.0, 90.0, 120.0, 150.0, and 180.0 s. To determine the effect of thermal postcure (after UV illumination) on the resulting thermal and mechanical properties, some specimens were postcured at 170°C in a laboratory oven for 2, 4, 6, and 8 h (the postcure time was measured to the nearest min).

The flexural strength and modulus of the photocured samples were determined using a United SFM-20 instrument in accordance with the ASTM D 790 method. The flexural properties were measured using the three-point flexural test with a span length of 50.8 mm (2 in.), a span-to-depth ratio of 16:1, a 454 kg (1000 lb) load cell, and a downdrive rate of 1.7 mm/min (0.07 in/min). Flexural strength and modulus values were calculated using DATUM 97 software (United Testing Systems).

2.3. Degree of cure

The degree of cure was determined using differential scanning calorimetry (DSC). In these experiments, cure was monitored by measuring the heat released by the sample as the exothermic reaction proceeded. The ultimate conversion achieved during a given set of cure conditions was determined by measuring the additional cure attained at an elevated temperature (180°C) after the completion of the specified cure cycle. Cure conditions that were investigated include: (A) photopolymerization for 2 min without the addition of a thermal initiator; (B) photopolymerization for 2 min without the addition of a thermal initiator, followed by postcure for 6 h at 170°C; (C) photopolymerization for 2 min with the addition of a thermal initiator; (D) photopolymerization for 2 min with the addition of a thermal initiator, followed by postcure for 6 h at 170°C. In each of these experiments, the photopolymerization was initiated at room temperature using the 3000 W Fusion Systems lamp without external heating or cooling. The temperature of 180°C was selected because it is higher than any temperature that the samples experienced during the cure cycles (and higher than the glass transition temperature of the samples) but lower than the degradation temperature of the cured PLEs.

Samples for the DSC experiments were prepared in the following manner. First, rectangular bars of the same dimensions as described above for the flexural tests were prepared according to the four different cure conditions. Four rectangular bars were prepared for each cure condition (all samples contained 74.0 wt.% fused silica). After the cure cycle was complete, a piece was cut from each rectangular bar and ground into smaller pieces with a mortar and pestle to prepare a sample for the DSC studies. The mass of each DSC sample was in the range of 18.0–25.0 mg. The samples were weighed both before and after the DSC cure experiment and no change in mass was observed for these solid samples.

The DSC experiments were performed using a Perkin Elmer DSC 7 Differential Scanning Calorimeter interfaced with a computer via the TAC 7/DX Thermal Analysis Instrument Controller. The Perkin Elmer Pyris Software package for Windows was used for the temperature control programs. The experimental procedure was as follows. A solid DSC sample weighing between 18.0 and 25.0 mg was placed in an aluminum DSC pan, which, in turn, was placed in the sample holder of the DSC instrument. An empty aluminum DSC pan was used in the reference holder. After the samples were placed in the DSC pans, the sample

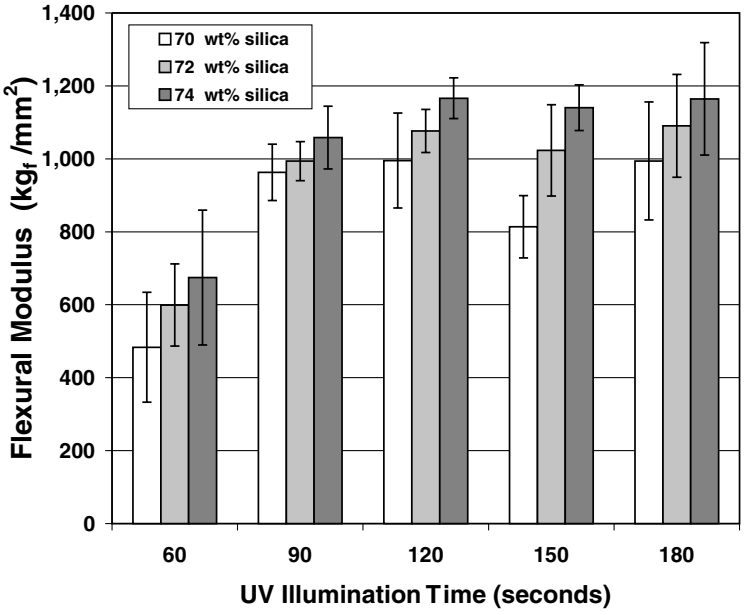

Fig. 1. Flexural modulus as a function of UV illumination time and filler loading.

cells were rapidly heated from 25 to 180°C by the DSC instrument. Once a temperature of 180°C was attained (in approximately 30 s) the instrument began to collect data for heat flow from the sample as a function of time. The heat flow was measured while the sample was maintained isothermally at 180°C for 150 min. It was generally observed that the heat flux from the sample ceased (indicating that the reaction was finished) in less than 20 min, therefore the duration of 150 min for the experiment was ample time to ensure that the reaction went to completion. For the analysis of the data, the values of the heat flux from the sample were normalized by the mass of the sample.

DSC experiments were also performed on the uncured liquid formulation containing 74.0 wt.% fused silica. These studies allowed the entire reaction exotherm corresponding to complete cure to be established. Four independent DSC runs were performed on the liquid formulation containing only the photoinitiator and four additional runs were performed on the liquid formulation containing both the photoinitiator and thermal initiator. In each of these experiments, a drop of the liquid formulation with a mass between 18.0 and 25.0 mg was placed in an aluminum DSC pan and an empty aluminum DSC pan was used in the reference holder. The heat flow was measured while the samples were maintained isothermally at 110°C for 250 min. A lower temperature was used for these studies to minimize evaporation of styrene in the resins. The samples were weighed both before and after the experiment to determine how much evaporation took place. The PLE samples with both photoinitiator and thermal initiator lost an average of 1.13% of their total weight, while the PLE samples with only the photoinitiator lost an average of 8.62% of their total weight. As will be shown in Section 3 of this paper, the liquid system without the thermal initiator did not polymerize at 110°C since the photoinitiator is stable at this temperature. This explains why more evaporation of the monomer was observed for this case. For the system containing both the photoinitiator and the thermal initiator, the final weight of the sample was used to normalize the heat flow data in the reaction exotherm profile.

2.4. Coefficient of thermal expansion and glass transition temperature

Specimens for coefficient of thermal expansion (CTE) testing were cut from the samples that had been used for flexural testing so that the thermal stress parameter of the photocured encapsulants could be estimated. The dimensions of the samples were 11.0 mm length × 8.0 mm width × 3.2 mm thickness. All samples were cut using a diamond wafering saw. The CTE below glass transition (α_1) and CTE above glass transition (α_2) were both measured using a DuPont 943 thermomechanical analyzer (TMA) interfaced with a DuPont model 9900 thermal analyzer controller. The samples were heated from room temperature (23°C) to 234°C at a constant rate of 3°C/min. The change in the sample thickness during heating was recorded in the personal computer and α_1 was obtained from the inclined line connecting two points on the TMA curve, 50 and 70°C. To determine α_2, the inclined line connecting 200 and 230°C was used. The glass transition temperature was taken to be the temperature at the intersection of these two lines.

All samples for CTE and glass transition temperature studies contained 70.0, 72.0, or 74.0 wt.% fused silica, 1.0 wt.% silane coupling agent (based on filler weight), 0.2 wt.% BAPO (based on resin weight), and the rest epoxy novolac-based vinyl ester resin. Samples with

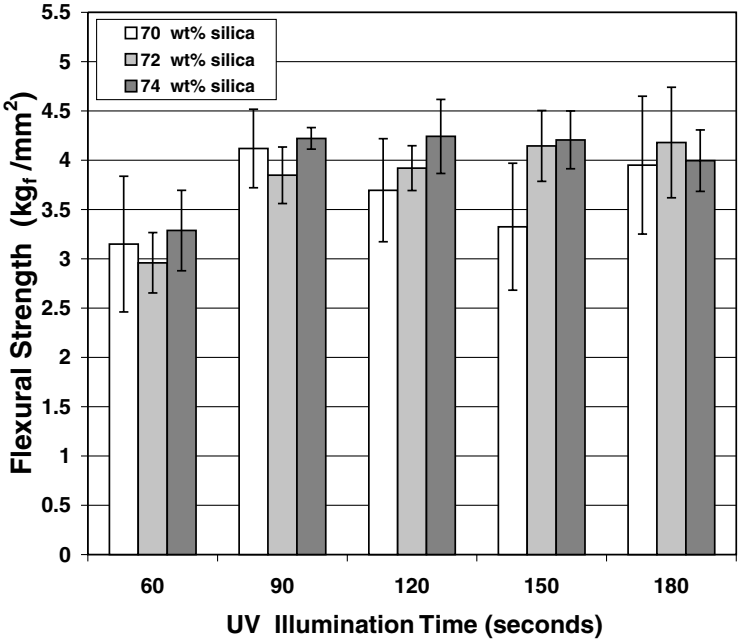

Fig. 2. Flexural strength as a function of UV illumination time and filler loading.

thermal initiator also contained 1.2 wt.% benzoyl peroxide (based on resin weight). All samples were photocured for 2 min with UV light of 200 mW/cm^2 UVA intensity and then postcured for 6 h at 170°C in a laboratory oven.

3. Results and discussion

3.1. Flexural strength and modulus

An important mechanical property for microelectronic encapsulants is the flexural modulus, which characterizes the stiffness of a material under an applied load [11]. The optimal value of the flexural modulus provides a balance between two conflicting requirements. A high value of the flexural modulus is desired to maximize the protection of the chip from an applied load; however, lower values of the flexural modulus lead to lower thermal stresses. Thermal stresses associated with high-modulus encapsulants can lead to failure of the microelectronic device. In particular, this stress has been reported to cause interfacial cracking and breakage of the wirebond leads, as well as passivation layer cracking and aluminum pattern deformation [12,13]. To reduce the thermal shrinkage stresses, while maintaining appropriate protection against mechanical shock, vibration, etc., a flexural modulus near 1000 kg$_f$/mm^2 (9800 MPa) is desired [5].

Experimental results for the effect of filler loading and UV illumination time on the flexural modulus and strength of the photocured encapsulants are shown in Figs. 1 and 2, respectively. In addition to the 70.0–74.0 wt.% fused silica, all samples contained 1.0 wt.% silane coupling agent (based on filler weight), 0.2 wt.% BAPO (based on resin weight), and the balance epoxy novolac-based vinyl ester resin, and were photocured with UV light of 200 mW/cm^2 UVA intensity. Each bar in these bar charts represents the average of five samples and the error bars indicate one standard deviation above and below the mean. As expected, the flexural modulus and flexural strength increase with fused silica content. In addition, the flexural properties do not change significantly as the illumination time is increased beyond 120 s. Therefore, 120 s was chosen for the in-mold illumination time for subsequent experiments. Note that the values of the flexural modulus are near the desired value of 1000 kg$_f$/mm^2. The results shown in Fig. 1 suggest that the PLEs could allow the in-mold cure time to be reduced significantly below 120 s (which is the typical in-mold cure time for transfer molding compounds). For example, the mechanical properties observed after 90 s are essentially equivalent to those after 120 s, and an ejectable hardness is certainly achieved even earlier. This result is significant because the in-mold cure time consumes approximately 70% of the overall cycle time and an in-mold cure time reduction of even 15 s can translate to a productivity increase of about 10% [5].

The data in Fig. 2 illustrate that the flexural strength of the samples as they are taken from the mold, immediately after illumination, range from 3 to 4.5 kg$_f$/mm^2 (~30–45 MPa). Current microelectronic encapsulants exhibit a flexural strength of at least 9 kg$_f$/mm^2 (after being postcured); therefore the strength of the PLEs immediately after illumination is below the range of desired values. To address this point, we investigated the effect of a postcure step (after photocuring the samples for 120 s with light of 200 mW/cm^2 UVA intensity) on the flexural strength and the flexural modulus. Most molding

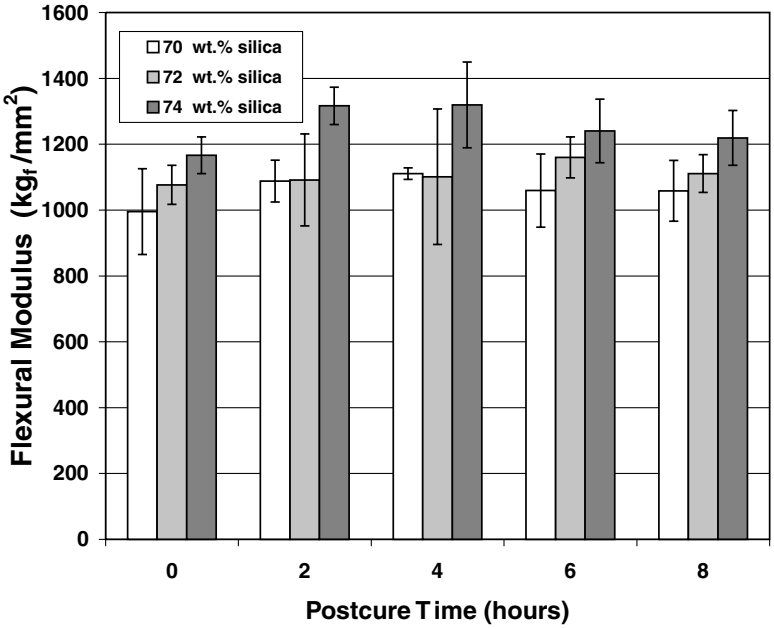

Fig. 3. Flexural modulus as a function of postcure time and filler loading.

compounds are postcured for 4–8 h at 170–175°C after the several-min cycle in the molding tool, in order to fully develop the material properties of the encapsulant. Postcuring is a key step in microelectronic encapsulation because encapsulated materials do not reach 100% chemical conversion during the transfer molding process. Typically, the reaction is continued in the mold until the encapsulant reaches a suitable ejectable hardness and then the encapsulant is postcured. The effect of postcure on the flexural properties is shown in Figs. 3 and 4 for a postcure temperature of 170°C.

The results shown in Figs. 3 and 4 illustrate that postcure has little effect on the flexural modulus, but has a significant impact on the flexural strength of the specimens. For example, a comparison of the flexural modulus data for no postcure to the data corresponding to 8 h of postcure, demonstrates that the values are not significantly different (for all three fused silica loadings, the mean flexural modulus and the associated standard deviations are nearly the same). In contrast, the flexural strength increases consistently as the postcure time is increased from 0 to 6 h. For

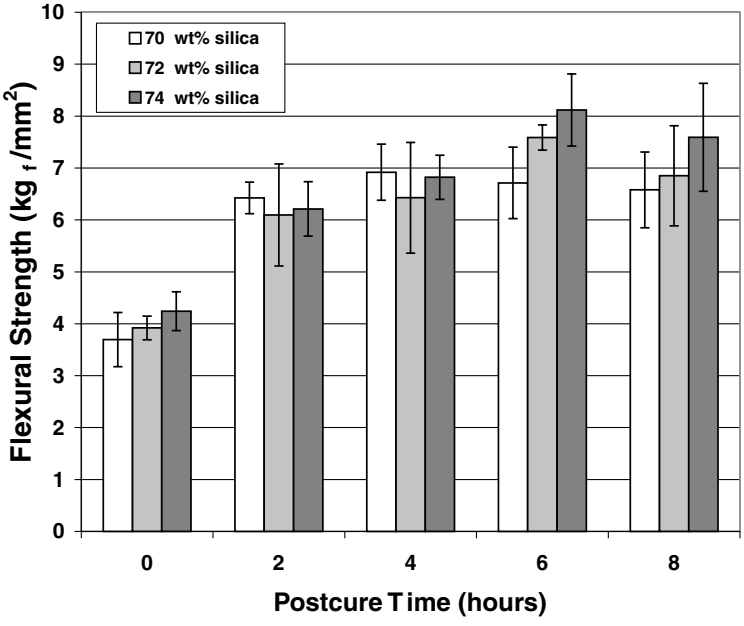

Fig. 4. Flexural strength as a function of postcure time and filler loading.

Table 1
Effect of the inclusion of thermal initiator on flexural strength of PLEs

Fused silica (wt.%)	Postcured?	Flexural strength (kg_f/mm^2)	
		Without thermal initiator	With thermal initiator
70.0	No	3.70 ± 0.52	5.25 ± 0.38
72.0	No	3.92 ± 0.23	5.50 ± 0.65
74.0	No	4.24 ± 0.38	5.71 ± 0.36
70.0	Yes	6.71 ± 0.69	8.83 ± 1.68
72.0	Yes	7.59 ± 0.24	9.28 ± 0.95
74.0	Yes	8.12 ± 0.69	9.92 ± 1.44

example, the samples filled with 74.0 wt.% fused silica exhibit an increase in the flexural strength from a value of 4 kg_f/mm^2 with no postcure to more than 8 kg_f/mm^2 after a postcure time of 6 h. We attribute the increase in flexural strength associated with the postcure step to additional thermal cure that occurs at the elevated temperatures, and possibly annealing of the polymer. A sample that has vitrified at room temperature can experience additional cure at elevated temperatures due to the enhanced molecular mobility that allows unreacted double bonds to encounter active centers. The enhancement in cure associated with the postcure step was characterized using differential scanning calorimetry, as explained later in this paper.

To investigate the effects of a dual photo/thermal initiation scheme, we included the thermal initiator, benzoyl peroxide, in addition to the photoinitiator BAPO in some PLEs. Table 1 illustrates the effect of the inclusion of the thermal initiator on the flexural strength of the resulting composites. The data in Table 1 correspond to samples that were UV cured for 120 s under a light intensity of 200 mW/cm^2. Samples that were postcured were done so for 6 h at 170°C after UV illumination. In addition to the fused silica at the indicated loading (70.0, 72.0, or 74.0 wt.%), all samples contained 1.0 wt.% silane coupling agent (based on filler weight), 0.2 wt.% BAPO (based on resin weight), and the balance epoxy novolac-based vinyl ester resin. Samples with thermal initiator also contained 1.2 wt.% benzoyl peroxide (based on resin weight). The flexural strength values reported in the tables are the average of five samples, and the indicated range corresponds to one standard deviation.

The data in Table 1 illustrate that the inclusion of the thermal initiator has a significant effect on the flexural strength of the cured encapsulants (for each filler loading, the flexural strength increased by approximately 2 kg_f/mm^2 upon the addition of the thermal initiator). As illustrated by the calorimetric studies described in the next section, the increase in the flexural strength can be attributed to an enhancement in the degree of cure associated with the addition of the thermal initiator. Moreover, a 6-h postcure step at 170°C also enhances the flexural strength of the encapsulants containing both the photoinitiator and thermal initiator. The flexural strength of the samples containing the thermal initiator and 72.0 or 74.0 wt.% fused silica (and postcured for 6 h) now fall in the range of typical flexural strength values for encapsulants.

The effect of the thermal initiator on the flexural modulus of the cured encapsulants is illustrated by the data in Table 2. The data illustrate that the values of the flexural modulus for the samples containing both the photoinitiator and thermal initiator are essentially equivalent to those for the samples containing only a photoinitiator. In addition, the values of the flexural modulus are close to the 1000 kg_f/mm^2 value recommended by Manzione for microelectronic encapsulants [5].

3.2. Degree of cure

The degree of cure was determined using DSC by measuring the heat released from the sample as the exothermic reaction proceeded. The ultimate conversion achieved during a given set of cure conditions was determined by measuring the additional cure attained at an elevated temperature after the completion of the specified cure

Table 2
Effect of the inclusion of thermal initiator on flexural modulus of PLEs

Fused silica (wt.%)	Postcured?	Flexural modulus (kg_f/mm^2)	
		Without thermal initiator	With thermal initiator
70.0	No	995.28 ± 130.20	939.12 ± 111.47
72.0	No	1076.50 ± 59.27	1051.48 ± 89.64
74.0	No	1166.24 ± 55.73	1121.40 ± 88.30
70.0	Yes	1059.24 ± 111.18	973.40 ± 89.13
72.0	Yes	1160.11 ± 62.23	1139.05 ± 123.83
74.0	Yes	1240.38 ± 96.62	1206.61 ± 116.55

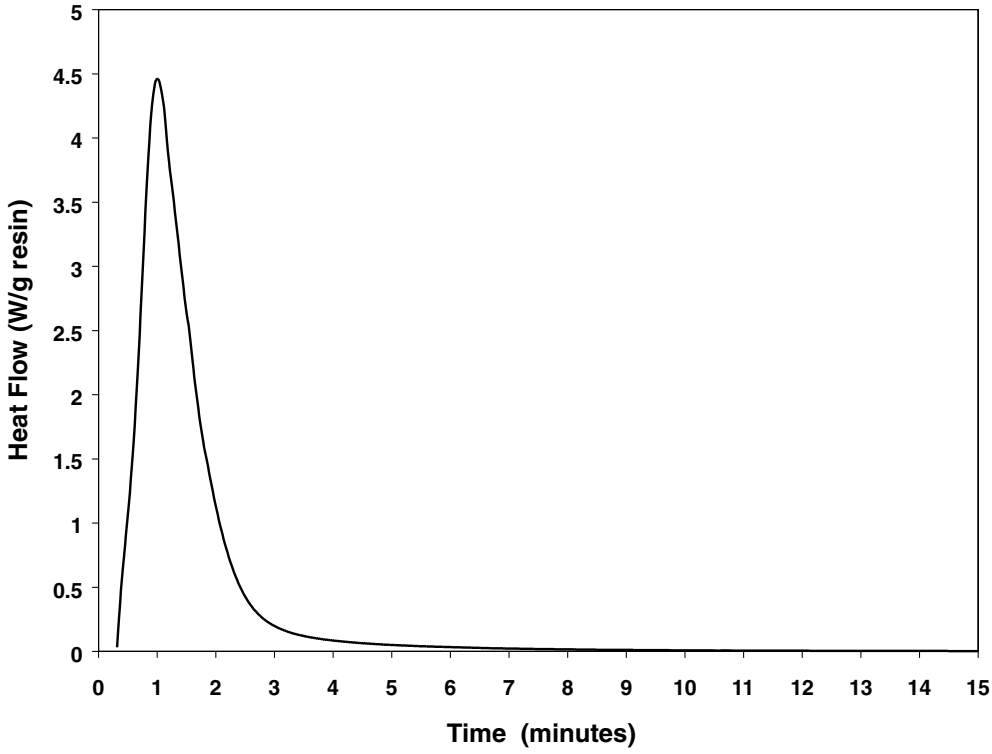

Fig. 5. Representative DSC reaction profile at 110°C for the liquid formulation containing 74.0 wt.% fused silica, 1.0 wt.% silane coupling agent (based on filler weight), 0.2 wt.% BAPO (based on resin weight), 1.2 wt.% benzoyl peroxide, and the balance epoxy novolac-based vinyl ester resin.

cycle. These experiments were performed to investigate the effect of postcure and the inclusion of the thermal initiator on the additional cure. To find the conversion attained during this additional cure, the heat released from the solid samples (that had gone through a given cure cycle) was divided by the heat released from the liquid formulation.

A representative reaction DSC profile for the uncured liquid formulation containing both the photoinitiator and thermal initiator is shown in Fig. 5. This figure contains a plot of the heat flow from the sample as a function of time and the reaction profile exhibits a shape that is characteristic of free radical polymerizations [14]. Since the polymerization reaction is exothermic, the area under this curve is proportional to the degree of cure. Although the data was collected for 150 min, the cure was generally complete (the profile becomes horizontal) in ~15 min, as illustrated in the figure. The baseline for integrating the area under the curve was established by horizontal extrapolation of the final steady-state value. The integration was performed using the commercial data analysis software package Origin 5.0 (Microcal Software, Inc.).

Cure conditions that were investigated in this study include: (A) photopolymerization for 2 min without the addition of a thermal initiator; (B) photopolymerization for 2 min without the addition of a thermal initiator, followed by postcure for 6 h at 170°C; (C) photopolymerization for 2 min with the addition of a thermal initiator; (D) photopolymerization for 2 min with the addition of a thermal initiator, followed by postcure for 6 h at 170°C. These samples will henceforth be referred to as A, B, C, and D, respectively. After the given cure cycle, each photopolymerized (solid) encapsulant was subjected to a DSC postbake at 180°C for 150 min. Based upon the heat released during this DSC postbake experiment, the degree of cure was determined indirectly by measuring the additional cure that could be attained at this elevated temperature. For a given solid sample, the additional degree of cure was determined by dividing the area under the corresponding DSC reaction profile by the area corresponding to complete cure. The latter value was obtained from the reaction exotherm exhibited by the previously unreacted liquid formulation (Sample E). The experimental data for samples containing

Table 3
Heat released during DSC postbake and additional cure for PLEs subject to various cure cycles

	Sample A	Sample B	Sample C	Sample D	Sample E
Heat released (J/g resin)	26.36 ± 0.97	2.80 ± 1.22	2.41 ± 0.58	1.02 ± 0.24	323.87 ± 11.91
Additional cure (%)	8.14	0.86	0.74	0.31	–

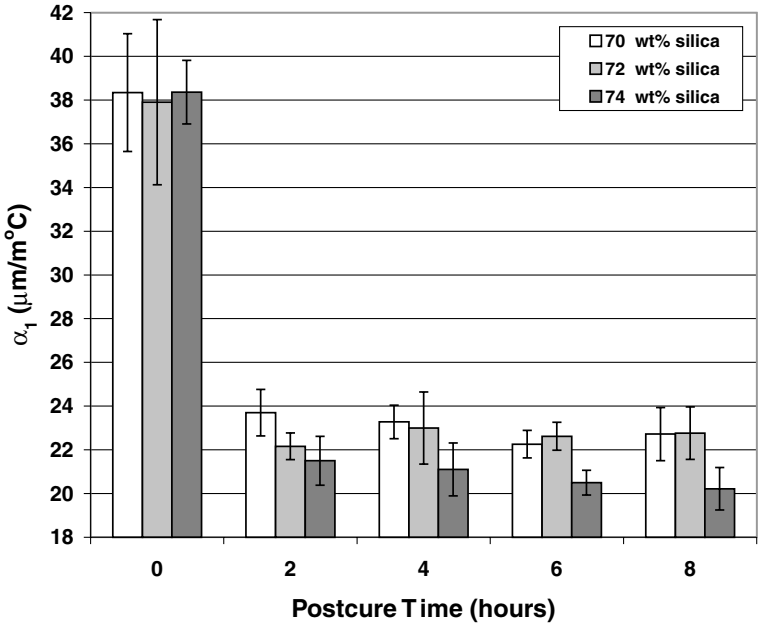

Fig. 6. CTE below glass transition as a function of postcure time and filler loading.

74 wt.% silica is shown in Table 3. The values in this table represent the average of four samples, and the indicated range corresponds to one standard deviation.

The data in Table 3 help to explain the effect of the cure cycle on the flexural strength that was identified in the previous section. Recall that flexural strength was enhanced by postcure and by the presence of the thermal initiator. The data in Table 3 illustrate that either of these factors leads to a significant enhancement in the conversion attained during the cure cycle (an enhancement of ~8%). For example, the effect of postcure is illustrated by comparing the data for Sample A to that for Sample B, while the effect of the inclusion of the thermal initiator is illustrated by comparing the data for Sample A to that for Sample C. Therefore, the enhanced flexural strength of these samples may arise from an increased degree of cure. The data for Sample D further illustrate that the highest degree of cure is obtained if a thermal initiator is included and the sample is subject to postcure. This is the sample that also exhibited the highest flexural strength; however, if Sample D is compared to Sample B or Sample C, it is unclear why the relatively small increase in conversion would lead to the relatively large increase in the flexural strength.

3.3. Coefficient of thermal expansion and glass transition temperature

The linear coefficient of thermal expansion (CTE) is defined as the ratio of the change in the length of the sample to the change in temperature per unit initial length [15]. This parameter is very important in semiconductor encapsulation because a significant CTE mismatch between the encapsulant, lead frame, and the silicon chip can lead to the build up of internal stresses in the microelectronic device, and could lead to cracking of the chip or encapsulant. Current encapsulants exhibit α_1 values (CTE below glass transition) in the range of 15–30 μm/(m °C), while copper lead frames possess a value of 16–17 μm/(m °C) and silicon exhibits a value of 3–4 μm/(m °C) [16]. The service temperature for microelectronic encapsulants is typically between 75 and 85°C, which is well below the glass transition temperature of the encapsulant [5]. For this reason, the value of the CTE above the glass transition temperature (α_2) is not as important as the CTE below the glass transition temperature (α_1).

For the PLEs, the experimental results for the coefficient of thermal expansion below glass transition are shown in Fig. 6. In addition to 70.0–74.0 wt.% fused silica, all samples contained 1.0 wt.% silane coupling agent (based on filler weight), 0.2 wt.% BAPO (based on resin weight), and the balance epoxy novolac-based vinyl ester resin. All samples were photocured for 2 min with UV light of 200 mW/cm^2 UVA intensity and then postcured at 170°C in a laboratory oven. The figure illustrates the effects of postcure time and fused silica loading on the observed CTE. Each bar in the following bar charts represents the average of 5 samples and the error bars indicate one standard deviation above and below the mean. The data illustrates that for all three filler loadings, a significant reduction in α_1 is observed after just 2 h of postcure. This reduced value of the CTE may be attributed to the enhanced cure (~8% additional cure as determined using calorimetry) associated with the postcure step. Most of this additional cure occurs within the first 2 h of postcure. After a 2-h postcure, all of the photocured samples exhibit α_1 values well within the range required for current encapsulants. As expected, α_1 decreased as the fused silica loading was

Table 4
Effect of thermal initiator on the CTE below glass transition of the PLEs

Fused silica (wt.%)	α_1 (μm/(m °C))	
	Without thermal initiator	With thermal initiator
70.0	22.26 ± 0.63	22.70 ± 1.10
72.0	22.62 ± 0.64	20.92 ± 0.54
74.0	20.50 ± 0.57	20.12 ± 1.41

Table 5
Effect of thermal initiator on the glass transition temperature of the PLEs

Fused silica (wt.%)	Glass transition temperature (°C)	
	Without thermal initiator	With thermal initiator
70.0	148 ± 2	150 ± 2
72.0	150 ± 4	151 ± 1
74.0	152 ± 3	150 ± 1

increased from 70.0 to 74.0 wt.%. The 74.0-wt.% silica system looks especially promising for microelectronic encapsulants because of its low α_1 value (~20 μm/(m °C)).

The effect of the inclusion of the thermal initiator on the value of α_1 is illustrated in Table 4. CTE values are the average of five samples, and the indicated range corresponds to one standard deviation. The data illustrate that the thermal initiator does not have any appreciable effect on the value of α_1.

The CTE above the glass transition temperature (α_2) was also measured as a function of filler loading and postcure time for systems containing only the photoinitiator, as well as, for systems containing both the photoinitiator and thermal initiators. The values for the samples postcured for 6 h and containing 70.0, 72.0, and 74.0 wt.% fused silica (and no thermal initiator) were 66.74 ± 3.45, 61.78 ± 1.70, and 56.68 ± 2.91 μm/(m °C), respectively. The values for the samples postcured for 6 h and containing 70.0, 72.0, and 74.0 wt.% fused silica (and both photoinitiator and thermal initiator) were 69.44 ± 1.30, 63.46 ± 2.37, and 59.24 ± 2.39 μm/(m °C), respectively. These values were essentially independent of both postcure and the presence of the thermal initiator.

To provide effective protection of the microelectronic device, an encapsulant must exist in the glassy state at the use temperature (~80°C). Commercial encapsulants typically exhibit glass transition temperatures in the range of 140–180°C. Fig. 7 shows experimental data for the glass transition temperature of the photopolymerized encapsulants as a function of the postcure time for samples containing 70.0, 72.0, and 74.0 wt.% fused silica. As expected, the glass transition temperature generally increases with increasing postcure time, and reaches a plateau in ~6 h, consistent with the previous results for the flexural strength and the CTE. The effect of the thermal initiator on the glass transition temperature is illustrated in Table 5. Glass transition temperatures are the average of five samples, and the indicated range corresponds to one standard deviation. The data illustrate that the samples exhibit glass transition temperatures appropriate for microelectronic encapsulants, and that the presence of the thermal initiator has little effect on the glass transition temperature.

3.4. Thermal stress parameter

As was mentioned previously, lowering the stress parameter leads to improved device reliability. The thermal

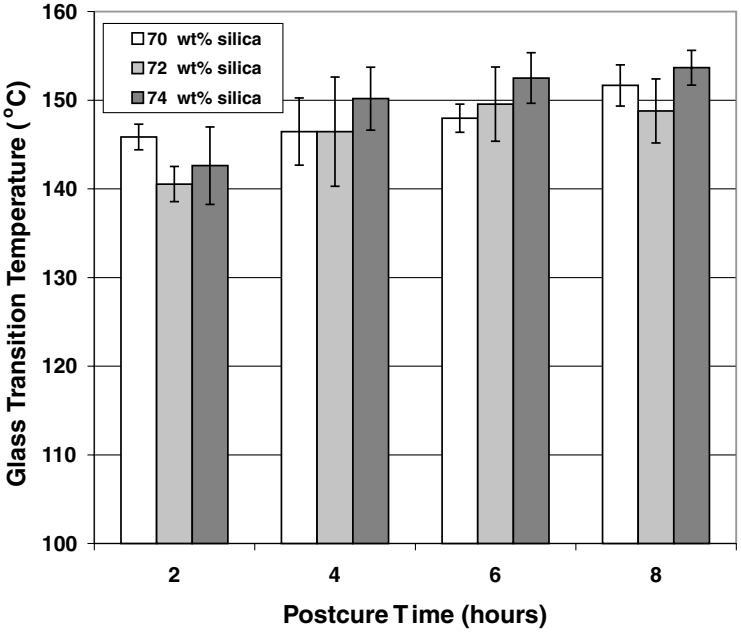

Fig. 7. Glass transition temperature as a function of postcure time and filler loading.

Table 6
Effect of thermal initiator on the thermal stress parameter of the PLEs

Fused silica (wt.%)	σ^* (kg_f/mm^2)	
	Without thermal initiator	With thermal initiator
70.0	1.34 ± 0.20	1.35 ± 0.32
72.0	1.58 ± 0.20	1.14 ± 0.23
74.0	1.13 ± 0.19	1.02 ± 0.47

stress parameter σ^* is typically calculated using the following equation [5]:

$$\sigma^* = (\alpha_{pg} - \alpha_i)E_{pg}(T_g - T_1) \quad (1)$$

Here α_{pg} represents the coefficient of thermal expansion below glass transition of the encapsulation material, α_i is the coefficient of thermal expansion of the silicon device or metal leadframe, E_{pg} the modulus of elasticity (tensile or flexural) of the encapsulant, and T_g the glass transition temperature of the encapsulant (°C). In order to evaluate the thermal stress parameter for the photopolymerized encapsulants of this study, the experimental values for α_{pg}, E_{pg} (flexural) and T_g were substituted into this equation along with literature values for α_i and T_1. Specifically, we used the CTE of a copper metal lead frame (16.3 μm/(m °C)) for α_i and −65°C for T_1, since this is the usual starting temperature for temperature cycling tests as specified by Mil. Std. 38510 Group D [5].

Calculated values for the thermal stress parameter of photopolymerized encapsulants with and without the thermal initiator are shown in Table 6. Thermal stress parameter values are the average of five samples, and the indicated range corresponds to one standard deviation. The data illustrate that the presence of the thermal initiator has little, if any, effect on the thermal stress parameter. More importantly, Table 6 illustrates that the photopolymerized encapsulants containing 74.0 wt.% fused silica exhibit a thermal stress parameter between 1.0 and 1.2 kg_f/mm^2. These values compare quite favorably to those reported for current encapsulants. For example, using the literature values for α_{pg}, E_{pg} (flexural) and T_g, reported by Nakamura et al. [17] and Lin et al. [18] along with the previously mentioned values for α_i and T_1, (16.3 μm/(m °C) and −65°C, respectively) current epoxy encapsulants exhibit a thermal stress parameter of ~1.3 kg_f/mm^2.

4. Conclusions

In this contribution, we have characterized the degree of cure, flexural strength, flexural modulus, coefficient of thermal expansion, glass transition temperature, and thermal stress parameter of novel photopolymerizable liquid encapsulants comprised of an epoxy novolac-based vinyl ester resin (~25 wt.%), fused silica (70–74 wt.%), and small amounts of a photoinitiator, silane coupling agent, and in some cases, a thermal initiator. In addition, we investigated the effect of the fused silica loading, UV illumination time, initiation scheme, and postcure time on these thermal and mechanical properties. The results indicate that a photocurable encapsulant loaded with 74.0 wt.% fused silica is very promising for this application since the aforementioned material properties meet or exceed those of current commercial encapsulants, while the viscosity is significantly reduced. These formulations are liquid at room temperature (current formulations are solid) and cure to an ejectable hardness in less than 2 min for an initiating light intensity of 200 mW/cm^2. The photocured samples exhibit appropriate values for the material properties after a postcure of 6 h. The photopolymerizable liquid encapsulants offer many advantages associated with low viscosity and potential for reduced in-mold cure times at room temperature. This reduction of the in-mold cure time could lead to significant productivity enhancements since the molding step plays a significant role in determining the production rate.

Acknowledgements

We are grateful for the financial and instrumental support from the Composite Materials and Structures Center (CMSC) at Michigan State University and, in particular, appreciate the help of Michael Rich and Phil Culcasi. Additional thanks go to Steve Beversluis of MINCO, Inc. for providing the fused silica, as well as, Scott Lindseth of Nitto Denko America, Inc. and Christine Naito of Dexter Electronic Materials for their help in answering specific questions about transfer molding compounds.

References

[1] Runyan WR, Bean KE. Semiconductor integrated circuit packaging. Reading, MA: Addison Wesley, 1990.
[2] Primeaux, F., Molded plastic package with wire protection, US Patent 5331205, 1994.
[3] McShane, M.B., Woosley, A.H., Primeaux, F., Method for encapsulating semiconductor devices with package bodies, US Patent 5344600, 1994.
[4] Han S, Wang KK. J Electron Packaging 1995;117:178.
[5] Manzione LT. Plastic packaging of microelectronic devices. New York, NY: Van Nostrand Reinhold, 1990.
[6] Narayanan V, Scranton AB. Trends Polym Sci 1997;5:415.
[7] Narayanan V, Baikerikar KK, Scranton AB. RadTech'98 North America UV/EB Conference Proceedings. p. 1998:31.
[8] Hanemann T, Ruprecht R, Haußelt JH. Polym Mater Sci Engng 1997;77:418.
[9] Baikerikar KK, Scranton AB. Polym Composites 2000;21(2):297.
[10] Bayer H, Lehner B. ACS Symp Ser 1990;417:412.
[11] Goosey MT. Plastics for electronics. New York, NY: Elsevier, 1985.
[12] Shin DK, Lee JJ. Adv Electronic Packaging (ASME) 1997;1:253.
[13] Ho TH, Wang CS. J Appl Polym Sci 1993;50:477.
[14] Scranton AB, Bowman CN, Klier J, Peppas NA. Polymer 1992;33(8):1683.
[15] Tummala RR, Rymaszewski EJ, editors. Microelectronics packaging handbook New York, NY: Van Nostrand Reinhold, 1989.
[16] Kinjo N, Ogata M, Nishi K, Kaneda A. Adv Polym Sci 1989;88:5.
[17] Nakamura Y, Yamaguchi M, Tanaka A, Okubo M. J Appl Polym Sci 1993;49:331.
[18] Lin LL, Ho TH, Wang CS. Polymer 1997;38:1997.